Differential Flatness Using the Predictive Neural Network Control Law for Hybrid Power System

Ilyes Tegani*‡, Abdenacer Aboubou*, Ramzi Saadi*, Mohamed Yacine Ayad**, Mohamed Becherif***

*Department of Electrical Engineering, University of Biskra, Laboratory of energy systems modeling, Algeria

** Industrial Hybrid Vehicle Applications, France

*** FCLab FR CNRS 3539 FEMTO-ST UMR CNRS 6174, UTBM Belfort, France

(tegani.ilyes@yahoo.fr, aboubou.nacer@gmail.com, ramzi_saadi2000@hotmail.fr, ayadmy@gmail.com, mohamed.becherif@utbm.fr)

‡Corresponding Author; Ilyes Tegani, Department of Electrical Engineering, University of Biskra, Laboratory of energy systems modeling, Algeria, Tel: +213 793 928 053, Fax: +213 793 928 0534567, tegani.ilyes@yahoo.fr

Received: 13.03.2015 Accepted:19.04.2015

Abstract- In this paper, a control design for a renewable energy hybrid power system that is fed by a photovoltaic (PV), Wind turbine (WT) and fuel cell (FC) sources with a battery (Batt) storage device is presented. The energy generated is managed through a nonlinear approach based on the differential flatness property. The control technique used in this work permits the entire description of the state's trajectories, and so to improve the dynamic response, stability and robustness of the proposed hybrid system by decreasing the static error in the output regulated voltage. The control law of this approach is improved using the predictive neural network (PNN) to ensure a better tracking for the reference trajectory signals. The obtained results show that the proposed flatness-PNN is able to manage well the power flow in a hybrid system with multi-renewable sources, providing more stability by decreasing the perturbation in the controlled DC bus voltage.

Keywords: Control; renewable energy; hybrid system; photovoltaic; Wind turbine; fuel cell; battery; flatness systems; neural network; energy management.

1. Introduction

Nowadays, the renewable power generation systems are expected to be increasingly used in different applications. The solar and the wind can be considered as effective and harmless energy sources; however, there are still some serious disquiets about these renewable energy sources and their employment. The solar and wind energies cannot produce power progressively, since its power production rates change with periods, months, days and hours. So the common disadvantage among these systems is their intermittent nature and dependence on weather changes. Therefore, such systems can be equipped with fuel cells as a secondary generation source and batteries bank devices for the storage reasons and to meet the requirement load demand during the system's lifetime. Usually, hybrid systems which contain more than one generation source can be considered as efficient systems, often two or more renewable energy sources are required to ensure a reliable and cost effective power [1].

A combination of PV, WT and FC sources forms a good production power system with promising features for distributed generation applications. Of course, the slow response of the FC [2] needs to be compensated with a storage system such as batteries or supercapacitors. A battery storage has been chosen in this work due to economic reasons.

Recently, an investigation of the literature has revealed that numerous researches have been performed for modelling with linear or nonlinear control features and in the various engineering disciplines for example; the control structure in micro grids with distributed generation: Island and grid-connected mode in [3], predictive control of the solid oxide fuel cell stack temperature with models based on experimental data [4]; control of electric power distributed generation systems for micro grid applications has been studied in [5], control of a mobile manipulator actuated by DC Motors in [6] and control of PEM fuel cell system via higher order sliding mode control in [7].

Furthermore, several approaches have been applied such as adaptive control [8, 9], exact linearization technique [8, 10, 11], self-tuning methods or sliding mode control [7], flatness control [12, 13] or fuzzy logic based-control [14, 15], have been widely studied for nonlinear power electronic applications. For modern control system, the flatness theory was announced by [16] in 1995. Recently, these concepts have been used in a diversity of nonlinear systems across the various engineering areas including: control of current-fed DC-DC converter in [17], control algorithm of Li-ion battery substation for DC distributed system in [18], and energy management of Stand-alone Photovoltaic/Wind Generator Systems in [19]. It is appropriate for robustness, predictive control, trajectory planning and constraints handling [20]. The flatness-based control is convenient in cases where an explicit trajectory generation is necessary. Another advantage of this technique is that when the flat output is used, the trajectory is controlled, and evolution of the trajectory of state, and control variables are well known even in transient state [21].

In this work, a differential flatness approach hybridized with the predictive neural network control algorithm for a PV/WT/FC power generation unit has been studied. A battery bank storage device has been employed. The next section describes the structural design of the hybrid generation system and modelling of the power plant. Section 3 presents the proposed energy management algorithm, the differential flatness theory in brief, the proof of the flat system for the proposed renewable energy power plant, the control laws and system stability. Moreover, Section 4 presents the simulation results that have been obtained, where a comparison between the two planning control laws has been analysed. Finally, the paper ends with concluding interpretations.

2. Structural Design and Description of the Hybrid System

2.1. Description of the proposed hybrid system

The model of the proposed hybrid PV–WT-FC-Battery power generation system contains photovoltaic arrays, wind turbine, Fuel cell and battery bank. Also the system involves IBC and buck-boost inverters, controllers for MPPT of PV panels and wind turbine. A demonstration diagram of the basic proposed hybrid system is shown in Fig.1.

The photovoltaic source, wind turbine and fuel cell distribute power to satisfy the load demand. As soon as the generated power by the PV-WT-FC sources meets the load demand, this energy will be oriented to supply the batteries until it is fully charged. In the other situation, when energy produced by PV-WT-FC sources is fewer than the load demand, the batteries will support the principal power sources by supplying the power lack until the energy stored in the batteries is depleted.

2.2. Power sources associated converters

The studied hybrid system comprises a 120 V DC bus for a standalone application supplied by a 1200 W PEM fuel cell; 1200W photovoltaic array power rating, 1000W of small scale wind turbine and a battery storage device of 100Ah.

The power sources operates giving direct current at an output voltage which; generally; is not appropriate with the chosen regulated DC bus voltage thus, interleaved boost converter (IBC) and buck-boost converter have been chosen to be associated with the power sources. The IBC converters presented in Fig. 2, is selected to adapt the output voltage of the power sources to the DC voltage and to decrease the current undulation, accordingly increase the efficiency of the hybrid system.

IBC converters are associated with the PV, WT and the FC power sources, in other hand we used a buck-boost converter to be associated with the batteries bank. The IBC has several advantages compared to the Conventional Boost converter due to the higher efficiency, lower voltage ripple, and lower ripple current and high reliability [22].

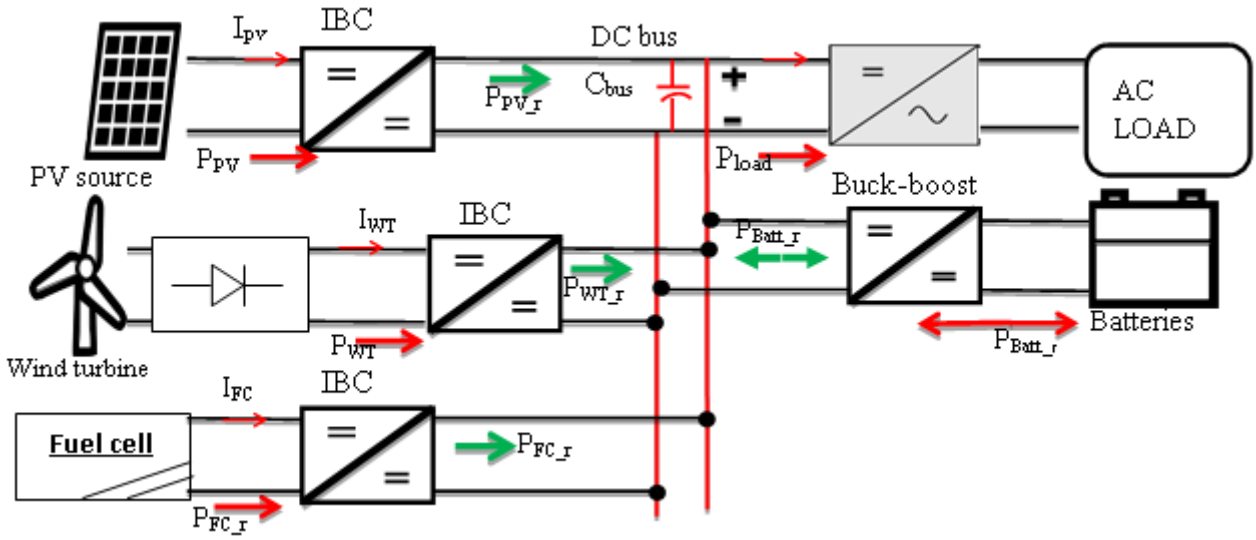

Fig. 1. Scheme of the basic proposed PV/WT/FC/Battery hybrid system.

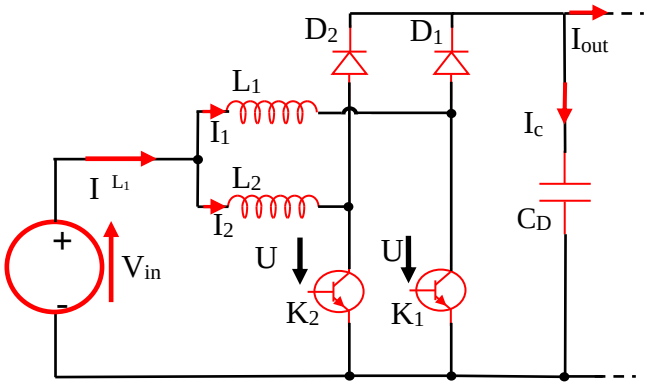

Fig. 2. Structure of the IBC converter.

The interleaving technique is widely used in the field power electronics where the voltage and current undulation can go beyond the handling capability of the system in high renewable power applications. Therefore, such systems can be equipped with IBC converters to handle the problem of current ripple.

In this study, a two-phase IBC converter has been used, consisting two parallel connected boost converter elements, and shifting drive by signals by 180°.

For two phase interleaved boost converter, two different modes of operation can be considered. At 0.5 the converter benefits from ripple elimination and input current ripple is zero, although output capacitor ripple is at their minimum. The timing signal is shown in fig 3.

For the Battery bank storage system, the buck-boost converter has been used (Fig 4.).

2.3. *The mathematical equations modelling the system*

The mathematical model of the DC-DC associated buck-boost, IBC converters, photovoltaic panel, fuel cell, wind turbine and the DC bus are given in equation (1).

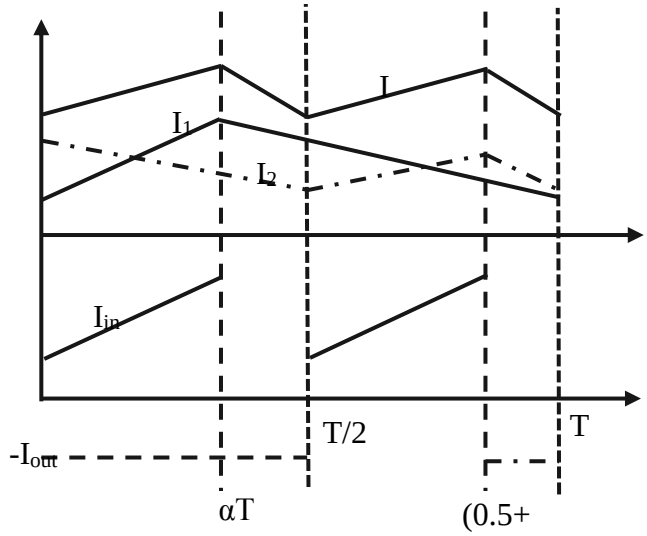

Fig. 3. The timing signal of the IBC.

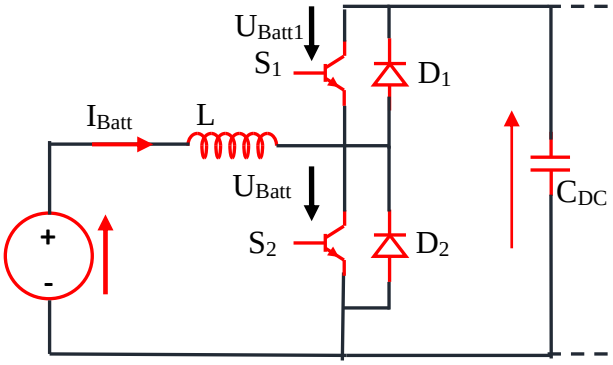

Fig. 4. The Structure of the buck boost battery associated converter.

$$\begin{cases} L_{Batt}\dfrac{dI_{Batt}}{dt} = V_{Batt} - (1-U_{Batt})V_{bus} - r_{Batt}I_{Batt} \\ V_{Batt} = E_0 - V_{cb} - R_{Batt}I_{Batt} \end{cases} \quad (1)$$

The model of the Lead-Acid battery used in this study is given in the Fig. 5.

Where the electrical model of the lead acid battery includes an electromotive force (E0) modelling the open circuit voltage of the battery, a capacitor (Cb) modelling the internal capacity of the battery and an internal resistance (Rs) [23].

The current of IBC converter associated with PV source can be modelled as follows:

$$\begin{cases} L_{1PV}\dfrac{dI_{1PV}}{dt} = V_{PV} - (1-U_{1PV})V_{bus} - r_{1PV}I_{1PV} \\ L_{2PV}\dfrac{dI_{2PV}}{dt} = V_{PV} - (1-U_{2PV})V_{bus} - r_{2PV}I_{2PV} \\ I_{PV} = I_{L1PV} - I_{L2PV} \end{cases} \quad (2)$$

Where the PV cell circuit model and equations can be obtained in equation (3).

$$\begin{cases} I_D = I_0(e^{V_D/V_T} - 1) \\ -I_D + I_{SC} - \dfrac{V_D}{R_P} - I_{PV} = 0 \\ V_{PVcell} = V_D - R_s I_{PV} \end{cases} \quad (3)$$

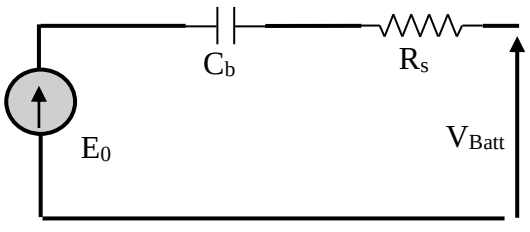

Fig. 5. R-C model of the lead-Acid battery.

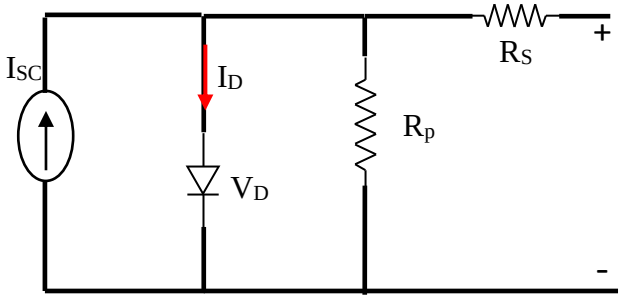

Fig. 6. Electrical model of a solar cell.

I_D, I_{SC}, R_p and R_s are the diode current, current of the solar cell, internal shunt resistance and the internal series resistance.

Hence, the V_{PV} can be obtained by the equation (4):

$$\begin{cases} V_{PV} = N_S V_{PVcell} \\ \mathrm{N_s} \text{ is the number of cells in series.} \end{cases} \quad (4)$$

The solar cell can be represented by the Fig. 6.

The current of IBC converter associated with FC source can be modelled by the equation (5):

$$\begin{cases} L_{1FC}\dfrac{dI_{1FC}}{dt} = V_{FC} - (1-U_{1FC})V_{bus} - r_{1FC}I_{1FC} \\ L_{2FC}\dfrac{dI_{2FC}}{dt} = V_{FC} - (1-U_{2FC})V_{bus} - r_{2FC}I_{2FC} \\ I_{FC} = I_{L1FC} - I_{L2FC} \end{cases} \quad (5)$$

In this work the Static model Proton Exchange Membrane fuel Cell (PEMFC) has been used [24]:

$$V_{FC} = E_0 - \overline{A}\,\log\left(\frac{i_{FC}-i_n}{i_0}\right) - \left\{\begin{matrix} R_m(i_{FC}-i_n + \\ \overline{B}\,\log(1-\dfrac{i_{FC}-i_n}{i_{Lim}}) \end{matrix}\right\} \quad (6)$$

Also, the current of IBC converter associated with WT power source can be written as follows:

$$\begin{cases} L_{1WT}\dfrac{dI_{1WT}}{dt} = V_{WT} - (1-U_{1WT})V_{bus} - r_{1WT}I_{1WT} \\ L_{2WT}\dfrac{dI_{2WT}}{dt} = V_{WT} - (1-U_{2WT})V_{bus} - r_{2WT}I_{2WT} \\ I_{WT} = I_{L1WT} - I_{L2WT} \end{cases} \quad (7)$$

The V_{WT} can be obtained via an AC/DC rectifier system using to adjust and regulate the produced voltage from the wind turbine.

DC link can be modelled by the equation (8).

$$\begin{cases} C_{bus}\dfrac{dV_{bus}}{dt} = -I_{Load} + (1-U_{Batt})I_{Batt} \\ +\left[(1-U_{1PV})I_{L1PV} + (1-U_{2PV})I_{L2PV}\right] \\ +\left[(1-U_{1FC})I_{L1FC} + (1-U_{2FC})I_{L2FC}\right] \\ +\left[(1-U_{1WT})I_{L1WT} + (1-U_{2WT})I_{L2WT}\right] \end{cases} \quad (8)$$

Where U_{Batt}, U_{PV}, U_{WT}, U_{FC} is the control variable of the battery, photovoltaic, wind turbine, fuel cell converters. I_{Batt}, I_{PV}, I_{WT}, I_{FC} are the currents of the battery, photovoltaic, wind turbine, fuel cell power sources respectively. And C_{bus} is the capacitor of the DC bus.

3. Flatness Control of the Proposed Hybrid Power System

The advantage of this approach is that the trajectories of the system are totally estimated by the trajectories of a flat output and its derivatives without including any differential equation. [16, 25]. Currently, these ideas have recently been used in a variety of nonlinear systems across different engineering disciplines such as the hybrid vehicle, Space Robot Control and hybrid renewable generation systems. Also the Flat systems are suitable in situations where clear trajectory generation is necessary. The flat systems comportment can be given by its output. So it is possible to design the desired trajectory of the outputs and determine the control system.

A system of conventional differential equations is assumed to be differentially flat if it can be modelled as follows:

$$\begin{cases} \dot{x} = f(x,u) \\ u = \left[u_1, u_2, \ldots, u_m\right]^T \; u \in R^m \\ x = \left[x_1, x_2, \ldots, x_n\right]^T \; x \in R^n \\ Y = \left[Y_1, Y_2, \ldots, Y_m\right]^T \; Y \in R^m \end{cases} \quad (9)$$

x is the vector of variables, u is the control input , Y is the vector of flat outputs, and $(n, m) \in N^2$.

The vector Y can be written as a function of x and u as follows [26]:

$$Y = \phi(x, u, \dot{u}, \ldots, u^{(s)}) \quad (10)$$

Where (s) is the determinate number of derivatives.

The vectors x and u can be expressed in using the vector of flat outputs Y and finite number of its derivatives as follows:

$$\begin{cases} x = \varphi(Y, \dot{Y}, \ldots, Y^{(r)}) \\ u = \psi(Y, \dot{Y}, \ldots, Y^{(r+1)}) \end{cases} \quad (11)$$

Where r is the predetermined number of derivatives.

There is no differential equation of the form:

$$\varsigma(Y,\dot{Y},..,Y^{(k)})=0 \tag{12}$$

Where k is a predetermined number of derivatives.

The vector of flat outputs *Y* and its derivatives offer the dynamics representation of the system, so that if the flat outputs profiles are known as a function of time, then we can get the profiles of all the states of system and the corresponding entries. This property is used to estimate the paths of flat outputs.

3.1. Planning of the energy regulation reference trajectory

One of the major advantages of the control using flatness theory, is the possibility to plan the all trajectories of the flat output. Knowing this trajectory, if the system is modelled without any error, gives the opportunity to know the evolution of the system state variables and control variables without integrating any differential equation.

For the proposed hybrid renewable system, it is supposed that the PV, WT, FC and battery currents track their reference signals impeccably. Therefore, the reference current can be given by the equations (13.14.15 and 16).

$$I_{PV}=I_{PVref}=\frac{P_{PV}}{V_{PV}}=\frac{P_{PVref}}{V_{PV}} \tag{13}$$

$$I_{FC}=I_{FCref}=\frac{P_{FC}}{V_{FC}}=\frac{P_{FCref}}{V_{FC}} \tag{14}$$

$$I_{WT}=I_{WTref}=\frac{P_{WT}}{V_{WT}}=\frac{P_{WTref}}{V_{WT}} \tag{15}$$

$$I_{Batt}=I_{Battref}=\frac{P_{Batt}}{V_{Batt}}=\frac{P_{Battref}}{V_{Batt}} \tag{16}$$

Where P_{PV}, P_{WT}, P_{FC} and P_{Batt} are the generated power from the PV-WT-FC-Battery hybrid system. r_{pv}, r_{wt} r_{fc} and r_{batt} represent the only static losses in the PV, WT, and the FC and battery converters respectively. V_{PV}, V_{WT}; V_{FC}, V_{Batt} and I_{PV}, I_{WT}, I_{FC}, I_{Batt} are the voltage and the current of the photovoltaic, wind turbine, fuel cell, battery sources respectively.

The energy Y_{bus} stored in the DC link and energy Y_{batt} can be given as follows:

$$Y_{bus}=\frac{1}{2}C_{bus}V_{bus}^2 \tag{17}$$

Also the energy stored in the battery bank can be given by the equation (18):

$$Y_{Batt}=\frac{1}{2}C_{Batt}V_{Batt}^2 \tag{18}$$

Consequently, the full electrostatic energy Y_{tot} stored in the DC bus capacitor C_{Bus} and in the battery C_{batt} can be written as:

$$Y_{tot}=Y_T=\frac{1}{2}C_{bus}V_{bus}^2+\frac{1}{2}C_{Batt}V_{Batt}^2 \tag{19}$$

As shown in Fig. 7, the DC link capacitive energy Y_{Bus} can be described using P_{PV_r}, P_{WT_r}, P_{FC_r} P_{Batt_r}, and P_{Load} by a differential equation.

The Energy Y_{bus} according to P_{pv_r}, P_{WT_r}, P_{FC_r} P_{batt_r} and P_{load}:

$$\dot{Y}_{bus}=P_{pv\_r}+P_{WT\_r}+P_{FC\_r}+P_{Batt\_r}-P_{load} \tag{20}$$

Where,

$$P_{PV\_r}=P_{PV}-r_{PV}\times I_{PV}{}^2=P_{PV}-r_{PV}\times\left(\frac{P_{PV}}{V_{PV}}\right)^2 \tag{21}$$

$$P_{WT\_r}=P_{WT}-r_{WT}\times I_{WT}{}^2=P_{WT}-r_{WT}\times\left(\frac{P_{WT}}{V_{WT}}\right)^2 \tag{22}$$

$$P_{FC\_r}=P_{FC}-r_{FC}\times I_{FC}{}^2=P_{FC}-r_{FC}\times\left(\frac{P_{FC}}{V_{FC}}\right)^2 \tag{23}$$

$$P_{Batt\_r}=P_{Batt}-r_{Batt}\times I_{Batt}{}^2=P_{Batt}-r_{Batt}\times\left(\frac{P_{Batt}}{V_{Batt}}\right)^2 \tag{24}$$

The power demanded by the load can be expressed by the equation (25):

$$P_{load}=V_{bus}.I_{load}=\sqrt{\frac{2Y_{bus}}{C_{bus}}}.I_{load} \tag{25}$$

Also the power delivered from the battery bank can be given by the equation (26):

$$P_{Batt}=\sqrt{\frac{2Y_{Batt}}{C_{Batt}}}.I_{Batt} \tag{26}$$

Thus, the reference trajectory planning of the energy regulation in DC bus, is shown in Fig. 12.

3.2. Flatness proof of the proposed PV-WT-FC Battery hybrid system

The flat outputs *y*, the control input variables *u* and the state variables *x* can be given as follows:

$$Y=\begin{bmatrix}Y_{bus}\\Y_{tot}\end{bmatrix}=\begin{bmatrix}Y_1\\Y_2\end{bmatrix} \tag{27}$$

$$u = \begin{bmatrix} P_{Batt} \\ P_{pvdemd} \end{bmatrix} = \begin{bmatrix} u_1 \\ u_2 \end{bmatrix} \quad (28)$$

$$x = \begin{bmatrix} V_{bus} \\ V_{Batt} \end{bmatrix} = \begin{bmatrix} x_1 \\ x_2 \end{bmatrix} \quad (29)$$

In this study, the photovoltaic source is considered to be the main and primary power source for the hybrid proposed system, where P_{pvdem} is the demanded power by the flatness control algorithm.

We adopt that the DC link electrostatic energy Y_{bus} of the system is constant and determined as a flat output Y_1. Therefore we can write:

$$\dot{Y}_{bus} = 0 = P_{PV\_r} + P_{WT\_r} + P_{FC\_r} + P_{Batt\_r} - P_{load} \quad (30)$$

Conversely, the total electrostatic energy Y_{tot} stocked in the DC link capacitor C_{bus} and in the battery bank is constant and determined as a flat output Y_2. We can write:

$$\dot{Y}_2 = 0 = P_{PV\_r} + P_{WT\_r} + P_{FC\_r} - P_{load} \quad (31)$$

The first stat variable DC link voltage $V_{bus} = x_1$ and the battery power (defined as a control input variable u_1) can be given by the algebraic equation (32):

$$x_1 = V_{bus} = \sqrt{\frac{2Y_{bus}}{C_{bus}}} = \varphi(Y_1) \quad (32)$$

Calculation of the control variables demonstrates that they are also the functions of the system output mechanisms and their derivatives. The control variables are given as follows:

$$u_1 = 2P_{BattLim}\left[1 - \sqrt{1 - \left(\frac{\dot{Y}_1 + i_{load}.\varphi_1(Y_1) - P_{FC\_r} - P_{PV\_r} - P_{WT\_r}}{P_{BattLim}}\right)}\right] \quad (33)$$

$$u_1 = \psi(Y_1, \dot{Y}_1) = P_{Battref} \quad (34)$$

Where P_{Batlim} can be defined by:

$$P_{\mathrm{BattLim}} = \frac{V_{Batt}^2}{4r_{Batt}} \quad (35)$$

$P_{BattLim}$ is the limited maximum power of the battery buck boost converter.

The battery voltage V_{Batt} (the second state variable x_2) and the PV power (defined as the second control input variable u_2) can be written by the algebraic function in Eq. (36):

$$x_2 = V_{bus} = \sqrt{\frac{2(Y_{tot} - Y_{bus})}{C_{Batt}}} = \varphi_2(Y_1, Y_2) \quad (36)$$

The second control variable is given by the equation (37):

$$u_2 = 2P_{totLim}\left[1 - \sqrt{1 - \left(\frac{\dot{Y}_2 + i_{load}.\varphi_1(Y_1)}{P_{totLim}}\right)}\right] \quad (37)$$

Where;

$$P_{totLim} = P_{PVLim} + P_{FCLim} + P_{WTLim} \quad (38)$$

Accordingly to the equations of control variables (u_1, u_2), the first and the second one, the system can be considered as a flat system.

3.3. Feedback asymptotic law control

To track the Y flat output at its Y_{ref} reference, we use the following feedback asymptotic control law [27, 28].

$$(\dot{Y}_{1ref} - \dot{Y}_1) + k_1(Y_{1ref} - Y_1) + k_2\int(Y_{1ref} - Y_1) = 0 \quad (39)$$

$$\dot{Y}_1 = \dot{Y}_{1ref} + k_1(Y_{1ref} - Y_1) + k_2\int(Y_{1ref} - Y_1) \quad (40)$$

$$\dot{Y}_2 = \dot{Y}_{2ref} + K_{21}(Y_{2ref} - Y_2) \quad (41)$$

Where, $k_{1,21}=2\zeta w_n$ and $K_2=w^2$.

The control variables (u_1, u_2) have been used to correct the trajectory of the proposed hybrid system, and ensure that the system track well the reference path.

The frequency and damping pulse are adjusted to the desired dynamics. Where K is a correction control parameter. Note that if the solar panels, wind turbine and fuel cell is unable to deliver the power necessary for the load, the battery will supply the difference.

3.4. The neural network predictive law control

The neural network architecture is often only partially imposed by the task which is being performed: inputs, status, and network outputs can be set according to the designer, and the type and connectivity of neurons, we use in this work hidden neurons networks hyperbolic tangent activation function, fully connected. But the number of neurons cannot be fixed, it is generally determined by an iterative procedure, and according to the success of learning, also there are systematic methods for selecting dynamic models.

Also, for the task of the training in a neural network, there are: Two sequences of numbers, a sequence applied to the external inputs, and a sequence corresponding to the desired values for the outputs.

The sequence of the external inputs consists of commands applied to the process, and the sequence of the desired output of outputs is measured in the process. The goal is to estimate the coefficients of the predictor network so that its outputs are "as close as possible" to those of the process.

For the principals of nonlinear system control, it is

important to have correct models. Because of the good approximating capacity of multi-layer perceptron networks, precise neural models of nonlinear procedures can be developed. Several control structures using neural models and inverse neural models have been established, and in this work the predictive neural network has been used to correct and track the trajectory path of the DC link energy regulation.

Neural model can be represented by three-layer artificial neural network of multi-layer perceptron networks type. The connection structure of the proposed predictive neural network control law is shown in Fig. 8. Where the control law uses direct neural model to predict future outputs for the DC bus energy regulation trajectory. This control variable is optimized in each step of control process, so that predicted value of output to reach reference value Y_{busref}.

On the other hand, Predictive control (or feedforward compensation and correction) is an advanced control technique of automatic. It aims to control complex industrial systems. The principle of this technique is to use a dynamic model of the process within the real-time controller to anticipate the future behaviour of the process. Predictive control is part of the internal model control techniques (BMI: Internal Model Controller).

Predictive control can be used to control complex systems with multiple inputs and outputs where simple PID controller is not sufficient. This technique is particularly useful when the systems have significant delays, inverted responses and numerous disturbances.

Predictive control realizes each controller sampling time the same steps:

- Calculation of varying predictions controlled to a time horizon N2 (Fig. 7.) through the internal model.
- Development of a reference path to follow.
- Calculation of future control law to be applied to the manipulated variables to a time horizon Nu (Fig. 7.).
- Only the first element of the calculated control law is applied to the system clock to the next shot.
- All these steps would then be repeated, it is the principle of the receding horizon.

Therefore, the neural network predictive controller uses a neural network model of a nonlinear plant to predict future plant performance. A plant performance over a specified future time horizon will be optimized using the control input which is calculated by the controller. The first step is to determine the neural network plant model [29].

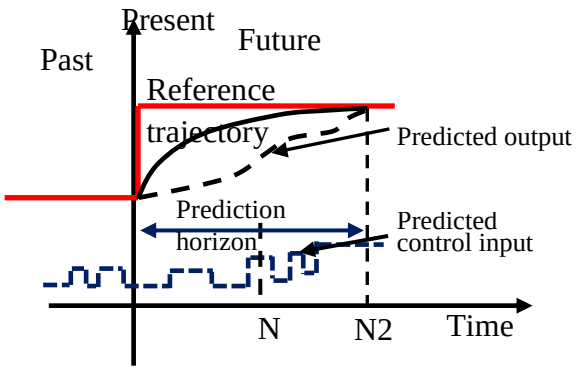

Fig. 7. Sequential predictive control chart.

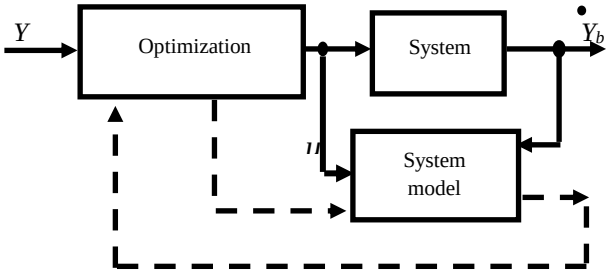

Fig. 8. Diagram of the neural network predictive control.

In this work the equation (42) describes the used plant model to predict the output of the control law:

$$\dot{Y}_{bus} = 0 = P_{PV\_r} + P_{WT\_r} + P_{FC\_r} + P_{Batt\_r} - \sqrt{\frac{2Y_{bus}}{C_{bus}}}.I_{load} \quad (42)$$

Where the scheme of the predictive neural network controller is shown in the Fig. 10.The input of the model plant is the energy of the DC link, the output of the controller model is the power which can be delivered from the DC bus.

The first step of the neural predictive control is to train a neural network to represent the forward dynamics of the plant. The estimate error between the plant output and the neural network output is used as the neural network training signal. The procedure is represented by the Fig. 8.The neural network plant model uses the energy of the DC link and previous plant outputs to predict future values (power which can be delivered from the DC bus). The topology of the used neural network model is given in the Fig. 9.Where W represents the weight of the neural network inputs. As it has been mentioned in the last section; the neural network model predicts the power delivered from the DC bus which is the plant response over a specified time horizon. The predictions are used by an arithmetical optimization algorithm to regulate the signal that minimizes the following performance condition over the identified horizon [30]:

$$J = \sum_{j=N_1}^{N_2} (Y_{bus}(t+j) - \dot{Y}_m(t+j))^2 + \rho \sum_{j=1}^{N_u} u(t+j-1) - u(t+j-2))^2 \quad (43)$$

Where N_1, N_2, and N_u (Fig. 7) define the horizons over which the tracking error and the control raises are calculated. The u variable is the tentative control signal, Y_{bus} is the desired response, and Y_m is the network model response. The

ρ value defines the influence that the sum of the squares of the control raises has on the performance index.

The structure of the whole controller system using the neural network predictive controller or the feedback asymptotic law control is given in the Fig. 10.

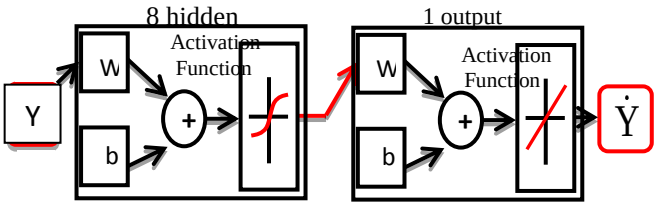

Fig. 9. Topology of the used neural network model.

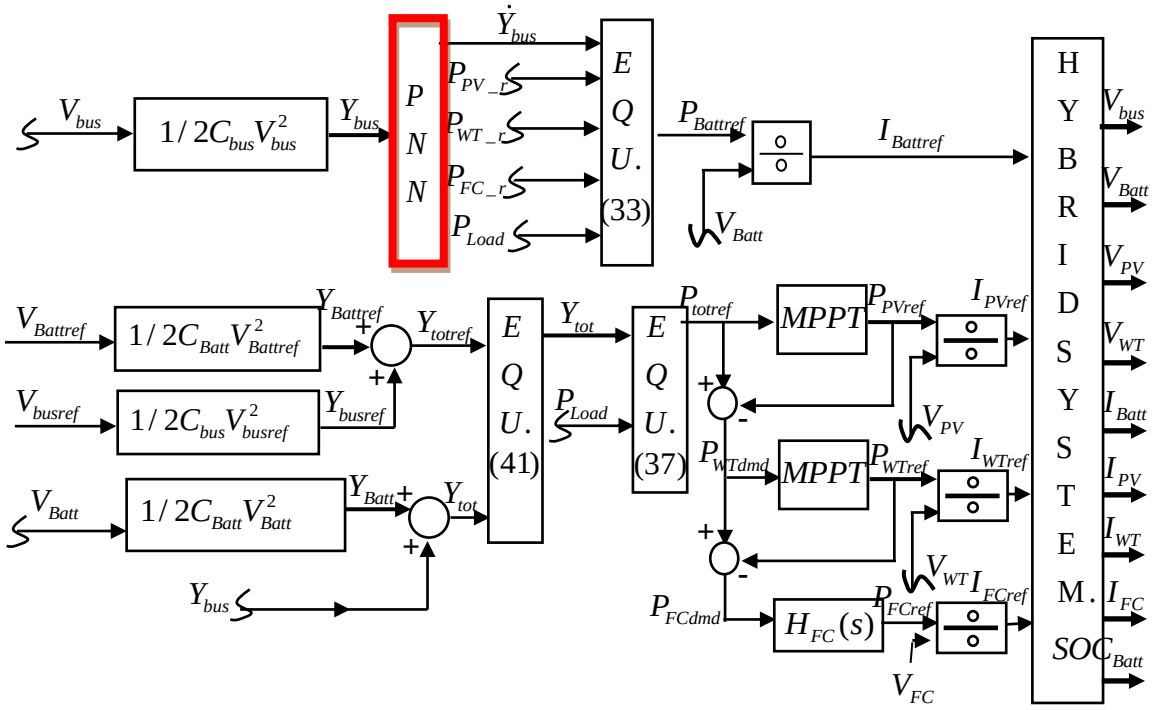

Fig. 10. Structural design control of the proposed hybrid system.

Fig. 10 illustrates the proposed control plan of the renewable PV-WT-FC-Battery system using the predictive neural network (PNN). The DC bus energy control law, which is the PNN, generates the reference signal as a power which can be delivered from the DC link. Then this power is divided by the measured voltage of the battery bank creating a battery current reference $I_{battref}$ by the equation (33). The total energy control law (the energy management of the whole system) generates a total power reference P_{totREF} (according to (41) and (37)). P_{totdmd} is then considered as the demanded photovoltaic power. Using maximum power point tracking algorithm (MPPT) the control system generates the reference power for the PV power source. Then, the algorithm calculates the difference between the total power reference P_{totREF} and the photovoltaic power reference P_{PVREF} to the WT power reference P_{WTREF}.

In the next step, the control algorithm calculates the difference between the P_{WTREf} and the P_{WTdmd} to assign the required power to the FC power source. A dynamics limitation have been used (given in (44)). The parameters related to the system energy regulation are summarized in Table 1, and 2.

A second order delay $H_{FC}(s)$ has been used as the FC power dynamic limitation is given by the equation (44):

$$H_{FC}(s) = \frac{1}{(\frac{s}{w_n}) + \frac{2\zeta}{w_n} s + 1} \quad (44)$$

Table 2. Parameters of battery bank.

Parameter	Nominal voltage (V)	Capacity (Ah)	Lifting range of voltage(V)	Internal resistance (Ω)
Value	48	100	58.8-42	0.0012

Table 1. Parameters of the renewable hybrid power sources

PV source parameter	Value	WT source parameter	Value	Fuel cell parameter	Value
STC power	300	Type	PMSG	Rated power (W)	1200

rating (W)					
Number of panels in parallel	4	Rated power (W)	1000	Rated current (A)	46
Panel open circuit voltage (V)	45.3	Rated voltage (V)	100	Rated voltage (V)	24
Panel rated voltage (V)	36.9	Rated current (A)	10	/	/
Panel rated current (A)	8.13	Starting speed (m/s)	2.5	/	/
Array rated power (W)	1200	Stopping speed (m/s)	35	/	/

4. Results and Comparison

The hybrid PV-WT-FC-Battery system is controlled through the closed loop of DC bus energy in two cases:

- Utilizing the asymptotic linearizing feedback control law.
- Utilizing the PNN control law.

However, the results of the energy management using the feedback asymptotic control law defined in the equation (40) are found similar to those when the PNN is used.

The results of the energy management can be given by the following figures:

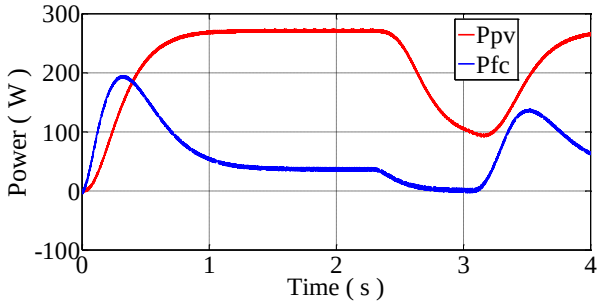

Fig. 11. Power produced from the PV and fuel cell sources.

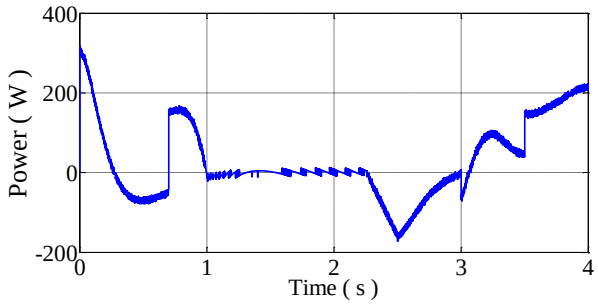

Fig. 12. Power produced from the battery bank.

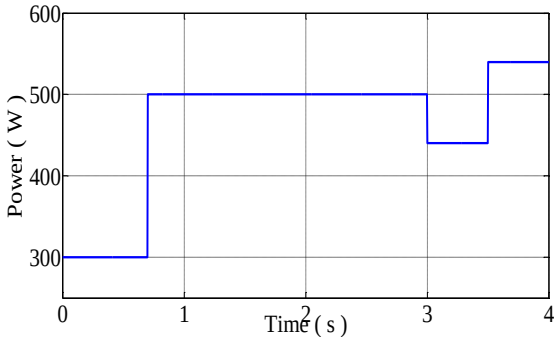

Fig. 13. The load profile.

We note that the power produced by the wind turbine due to the used wind speed profile.

From the 0 to 0.3s, the battery provides power to satisfy the load demand, on the other hand the PV system, which is the primary source, starts to generate power according to its irradiation data. The FC source, which is the secondary source, generates the needed power to cover the amount required during the functioning of the hybrid system, when the power generated from the wind turbine is zero due to the used wind speed.

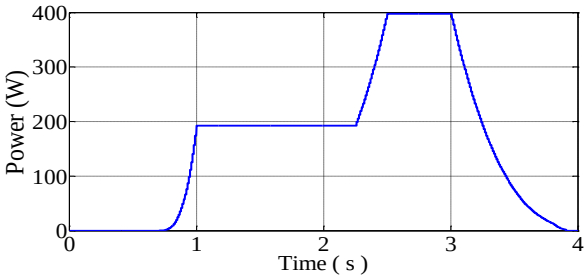

Fig. 14. The wind turbine produced power.

At 0.8s the wind turbine starts to deliver power, supplies the amount and supports the power generated from the photovoltaic source. In this stage the power of the fuel cell is decreased to zero.

The DC bus voltage, when the loop of DC bus energy regulation is controlled utilizing the asymptotic linearizing feedback is demonstrated in the Fig. 15.

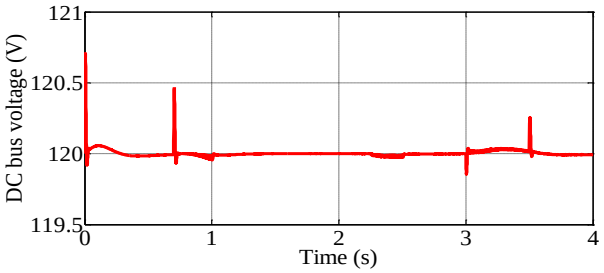

Fig. 15. The DC bus voltage using the asymptotic control law (equation 40).

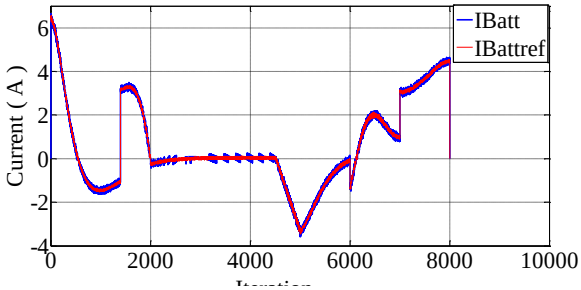

Fig. 16. The battery current and its reference.

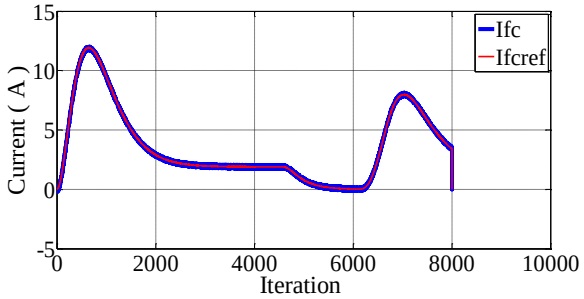

Fig. 17. The fuel cell current and its reference.

According to the Fig. 16 and 17, the current of the battery and Fuel cell track well its reference.

The voltage of the fuel cell and battery bank respectively are given as follows:

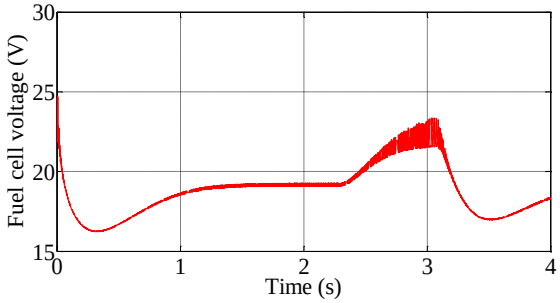

Fig. 18. The PEM fuel cell voltage.

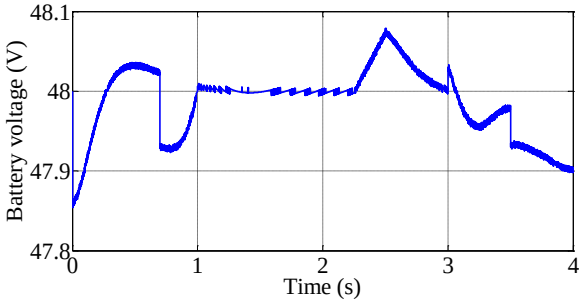

Fig. 19. Voltage of the battery.

The state of charge of the storage system is given as follows:

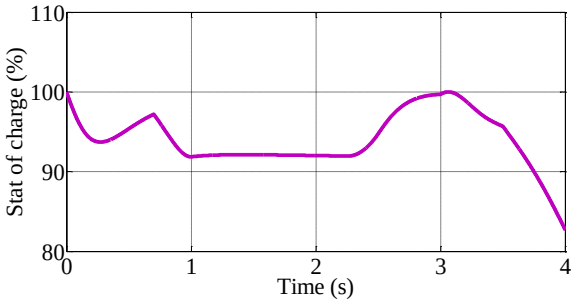

Fig. 20. The Battery bank state of charge.

In the second case, the loop of DC link energy regulation used the PNN controller. The first step is the validation of the plant model given in the equation (42). To control the predictive horizons, the following parameters have been applied:

N_2=7, N_u=2, and N_1 is fixed at 1. The weighting parameter ρ is assigned to 0.05. The parameter α serves to control the optimization which is fixed at 0.001. It defines how much reduction in performance is necessary for a successful optimization.

The results of the training, test and validation are demonstrated in figures (21, 22 and 23).

Where the input of the plant model is the energy of the DC link, and the output is the power which can be delivered from the DC link.

The results of the training , testing and validation data of the PNN controller denote that the plant model used in the controller is well modelled to predict the future output of the PNN controller (regulation of the DC bus voltage).

The training performance of the neural network is provided by the Fig. 24.

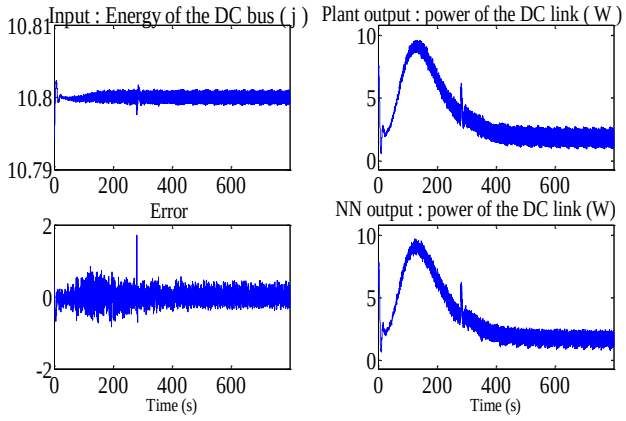

Fig. 21. Training results of the neural network plant model.

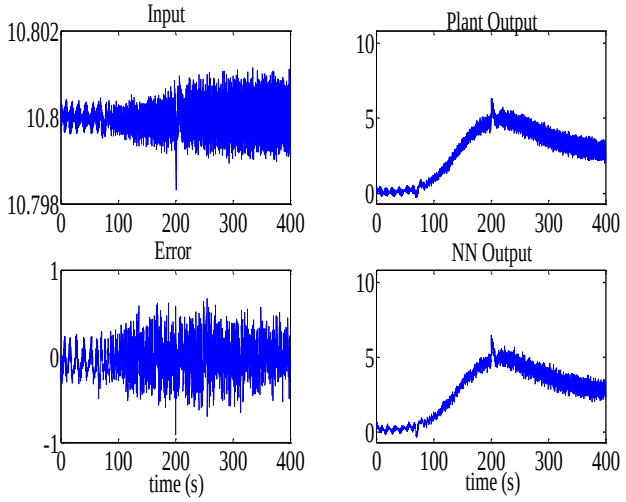

Fig. 22. Testing results of the neural network plant model.

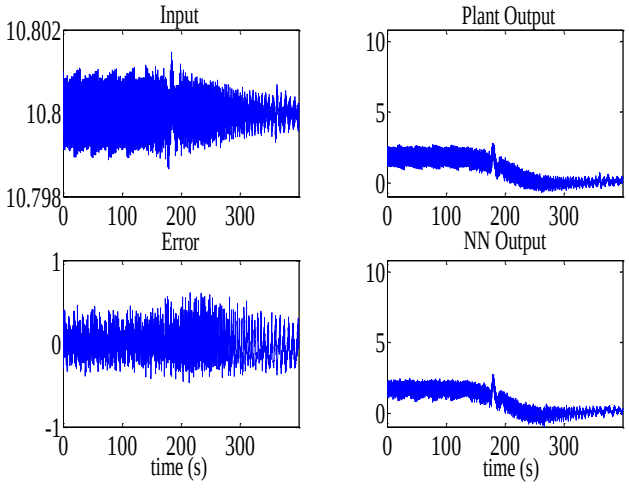

Fig. 23. Validation results of the neural network plant model.

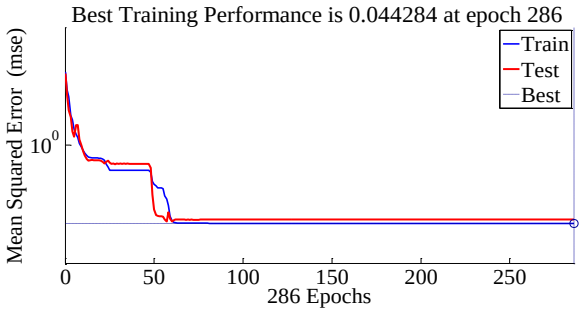

Fig. 24. Training performance of the neural network.

Where the best training performance is 0.044284 obtained at epoch 286.

The DC bus voltage of the second case (PNN law control) is given as follows:

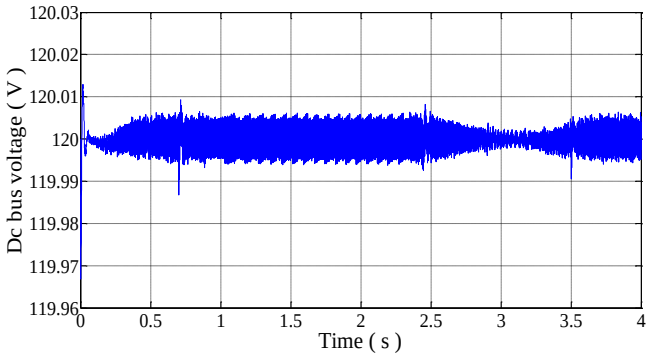

Fig. 25. The DC bus voltage using the PNN as a control law.

The Figure 15 and 25 show that both the control law algorithm using the predictive neural network and the asymptotic linearizing feedback modelled in the equation (40), track well the reference trajectory and conserve the DC bus voltage within their $V_{busref}=120V$. However, the static error has been decreased when the control system used the predictive neural network. Where a remarkable voltage change in T=0.8, 3,3.5s due to the load power demand variation is obtained when the asymptotic linearizing feedback given in the equation (40) has been used. The changing in voltage of the DC bus when the PNN has been used doesn't cross 0.98V = 0.8167%. Also, a chattering phenomenon is observed due to the current control of the power sources, where the sliding mode has been used.

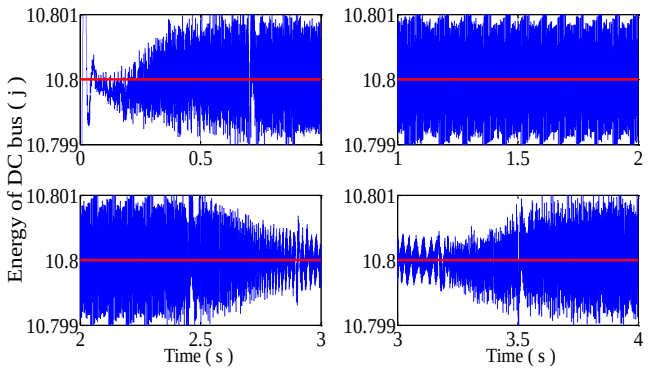

Fig. 26. The DC bus energy and its reference.

5. Conclusion

In this paper, an algorithm for control design of stand-alone PV-WT-FC-Battery system has been presented, based on the flatness control using both, a linearizing feedback asymptotic control law (given in equation 40) and the predictive neural network control law. The results of the proposed algorithms show that the planning control using the predictive neural network permits to regulate the energy of the DC link supplied for diverse loads with a lower static error, which provides more stability for the generation system. The system supports the control of power flow at the interface between the solar panel, wind turbine, fuel cell and the battery.

This technique increases the reliability of the system, controlling the power flow and holding power management. Furthermore, in this analysis, a design method was given. Where, the PV is the principal source, WT is the secondary source, while the FC works as a support source (backup generator source) to cover for the uncertainties of the PV source and The WT in case of load requirement, the battery bank serves as a storage device to compensate for the uncertainties of the PV, WT and FC generator sources in the steady state and transient state. This method does not necessitate a switching algorithm control, what is the main advantage to manage energy in hybrid power systems. With flatness based control using the predictive neural network as a control law, it is possible to operate the battery in different stages, charging or discharging, and whatever the variation of the load profile is, providing more stability and reliability of the system by decreasing the perturbation in the DC bus.

References

[1] C. Wang and M.H. Nehrir, "Power management of a stand-alone wind/photovoltaic/fuel cell energy system". Energy conversion, ieee transactions on, 2008. 23(3): p. 957-967.

[2] P. Thounthong, S. Rael, and B. Davat, "Energy management of fuel cell/battery/supercapacitor hybrid power source for vehicle applications". Journal of Power Sources, 2009. 193(1): p. 376-385.

[3] O. Palizban and K. Kauhaniemi, "Hierarchical control structure in microgrids with distributed generation: Island and grid-connected mode". Renewable and Sustainable Energy Reviews, 2015. 44: p. 797-813.

[4] A. Pohjoranta, et al., "Model predictive control of the solid oxide fuel cell stack temperature with models based on experimental data". Journal of Power Sources, 2015. 277: p. 239-250.

[5] A.M. Bouzid, et al., "A survey on control of electric power distributed generation systems for microgrid applications". Renewable and Sustainable Energy Reviews, 2015. 44: p. 751-766.

[6] A. Karray and M. Feki, "Adaptive and sliding mode control of a mobile manipulator actuated by DC motors". International Journal of Automation and Control, 2014. 8(2): p. 173-190.

[7] S.M. Rakhtala Rostami, A. Ranjbar Noei, and R. Gaderi, "Control of PEM fuel cell system via higher order sliding mode control". International Journal of Automation and Control, 2012. 6(3): p. 310-329.

[8] K.E. Johnson, et al., "Control of variable-speed wind turbines: standard and adaptive techniques for maximizing energy capture". Control Systems, IEEE, 2006. 26(3): p. 70-81.

[9] R. Marino and P. Tomei. *Adaptive Control of Stepper motors via nonlinear extended matching*. in *IF AC Workshop on Motion Control for Intelligent Automation*. 2014.

[10] A. Luviano-Juárez, J. Cortés-Romero, and H. Sira-Ramírez, "Trajectory Tracking Control of a Mobile Robot Through a Flatness-Based Exact Feedforward Linearization Scheme". Journal of Dynamic Systems, Measurement, and Control, 2015. 137(5): p. 051001.

[11] T. Taniguchi, L. Eciolaza, and M. Sugeno. *Model Following Control of a Unicycle Mobile Robot via Dynamic Feedback Linearization Based on Piecewise Bilinear Models*. in *Information Processing and Management of Uncertainty in Knowledge-Based Systems*. 2014. Springer.

[12] M. Aimene, A. Payman, and B. Dakyo. *Management of the wind turbine energy delivered to the grid based on the flatness control method*. in *Energy Conversion Congress and Exposition (ECCE), 2014 IEEE*. 2014. IEEE.

[13] I. Tégani, et al., "Optimal sizing design and energy management of stand-alone photovoltaic/wind generator systems". Energy Procedia, 2014. 50: p. 163-170.

[14] M.P. Lalitha, T. Janardhan, and R.M. Mohan. *The future of fuzzy logic based wind energy conversion system with solid oxide fuel cell and the passions of radical pedagogy*. in *Computational Intelligence on Power, Energy and Controls with their impact on Humanity (CIPECH), 2014 Innovative Applications of*. 2014. IEEE.

[15] S. Jie, Z. Yong, and Y. Chengliang, "Longitudinal brake control of hybrid electric bus using adaptive fuzzy sliding mode control". International Journal of Modelling, Identification and Control, 2012. 15(3): p. 147-155.

[16] M. Fliess, et al., "Flatness and defect of non-linear systems: introductory theory and examples". International journal of control, 1995. 61(6): p. 1327-1361.

[17] M. Phattanasak, et al. *Current-fed DC-DC converter with Flatness based control for renewable energy*. in *Electrical Engineering/Electronics, Computer, Telecommunications and Information Technology (ECTI-CON), 2014 11th International Conference on*. 2014. IEEE.

[18] S. Sikkabut, et al. *A nonlinear control algorithm of Li-ion battery substation for DC distributed system*. in *Power Electronics, Electrical Drives, Automation and*

Motion (SPEEDAM), 2014 International Symposium on. 2014. IEEE.

[19] P. Thounthong, et al. *Differential flatness control approach for fuel cell/solar cell power plant with Li-ion battery storage device for grid-independent applications*. in *Power Electronics, Electrical Drives, Automation and Motion (SPEEDAM), 2014 International Symposium on*. 2014. IEEE.

[20] P. Thounthong, "Model based-energy control of a solar power plant with a supercapacitor for grid-independent applications". Energy conversion, ieee transactions on, 2011. 26(4): p. 1210-1218.

[21] P. Thounthong, S. Rael, and B. Davat, "Analysis of supercapacitor as second source based on fuel cell power generation". Energy conversion, ieee transactions on, 2009. 24(1): p. 247-255.

[22] A.A. Bakar, et al. *DC-DC interleaved boost converter using FPGA*. in *Clean Energy and Technology (CEAT), 2013 IEEE Conference on*. 2013. IEEE.

[23] O. Gergaud, *Modélisation énergétique et optimisation économique d'un système de production éolien et photovoltaïque couplé au réseau et associé à un accumulateur*, 2002, École normale supérieure de Cachan-ENS Cachan.

[24] J. Larminie, A. Dicks, and M.S. McDonald, Fuel cell systems explained. Vol. 2. 2003: Wiley New York.

[25] B. Laroche, P. Martin, and N. Petit, "Commande par platitude. Equations différentielles ordinaires et aux dérivées partielles". 2008.

[26] F. Antritter and J. Lévine, *Flatness characterization: Two approaches*, in *Advances in the Theory of Control, Signals and Systems with Physical Modeling*2011, Springer. p. 127-139.

[27] A. Payman, "Contribution à la Gestion de l'Energie dans les Systèmes Hybrides Multi-sources Multi-charges". PhDthesis, Polytechnic Institute of Lorraine, Nancy, France, 2009.

[28] A. Payman, S. Pierfederici, and F. Meibody-Tabar, "Energy control of supercapacitor/fuel cell hybrid power source". Energy Conversion and Management, 2008. 49(6): p. 1637-1644.

[29] D.V.M. S.Angelin. *Optimal Operation of Power in Renewable Energy by Using prediction in Recurrent Neural Network, International Journal of Innovative Research in Computer and Communication Engineering*. [cited 2015 06/04/2015]; Available from: http://www.mathworks.com/help/nnet/ug/design-neural-networkpredictive-controller-in-simulink.html.

[30] M. Sedighizadeh, M. Rezaei, and V. Najmi, "A Predictive Control based on neural network for Proton Exchange Membrane Fuel Cell". World Academy of Science, Engineering and Technology, 2011.